Archives of Mechanics • Archiwum Mechaniki Stosowanej • 26, 2, pp. 229–241, Warszawa 1974

Interaction of material damping and monogenic-polygenic forces in viscoelastic system

R. N. KAPOOR (TORONTO) and H. H. E. LEIPHOLZ (WATERLOO, CANADA)

IN GENERAL, the elastic systems are always damped and possess polygenic as well as monogenic loads. Selecting a system, for which the authors have already shown the material damping to change the mode of instability from flutter to divergence, a detailed study is made of the interaction between the ratio of the two types of loads and the material damping. The results, obtained here, attain added significance in view of the increasing use of damping coatings and materials with high energy absorbtion coefficients in turbine blades, machine tools, aircraft components and several other systems, where the monogenic and polygenic forces invariably exist.

Układy sprężyste są z reguły tłumione i zawierają obciążenia typu poligenicznego jak i monogenicznego. Opierając się na układzie, dla którego autor wykazał już, że tłumienie materiałowe zmienia charakter wyboczenia z flatteru na dywergencyjny, przeprowadzono szczegółową analizę współdziałanie między stosunkiem tych dwóch rodzajów obciążeń oraz tłumieniem materiałowym. Otrzymane wyniki mają istotne znaczenie wobec wzrastającego zastosowania materiałów wibroizolacyjnych o wysokich współczynnikach pochłaniania energii do konstrukcji łopatek turbinowych, obrabiarek, konstrukcji lotniczych oraz wielu innych układów, w których niezmiennie występują siły poligeniczne i monogeniczne.

Упругие системы как правило обладают затуханием и содержат нагрузки так полигенного, как и моногенного типов. Опираясь на систему, для которой раньше автор показал, что материальное затухание изменяет характер продольного изгиба из флаттера в дивергентный, проведен подробный анализ взаимодействия между отношением этих двух типов нагрузок и материальным затуханием. Полученные результаты имеют существенное значение из-за возрастающего применения вибро-изоляционных материалов с высокими коэффициентами поглощения энергии для конструкции турбинных лопаток, станков, авиационных конструкций, а также многих других систем, в которых неизменно выступают полигенные и моногенные силы.

1. Introduction

IN THE STUDY of systems possessing monogenic as well as polygenic [1] forces, one field of research has been the investigation of conditions under which the mode of instability may change from flutter to divergence or *vice-versa*. DZHANELIDZE [2], KÖNIG [3], CONTRI in [4], HERRMANN and BUNGAY [5], ŻYCZKOWSKI and GAJEWSKI [6], and HUSSEYIN and PLAUT [7] have, by taking various undamped mathematical models, shown that depending on the ratio of the two types of forces, instability may occur in the form of either flutter or divergence. BOLOTIN and ZHINZHER [8] considered a viscoelastic cantilever with subtangential end force and obtained a similar result. The authors [9, 10] extended the investigation to a class of viscoelastic systems acted upon by a more general type of monogenic and polygenic forces and studied the combined influence of the load distribution pattern, material damping, as well as the ratio of the two types of forces. It was shown that for

a prescribed pattern of load distribution, the material damping could change a flutter system into a divergence system. If the load distribution pattern was otherwise, the mode of instability remained insensitive to damping. By taking a system, Fig. 1, with the appropriate value of n such that it falls in the former category, the object of this paper is to study, in detail, the interaction between ξ, the ratio of the monogenic and polygenic forces, and γ, the damping coefficient of the Kelvin-Voigt material. It is shown that the influence of γ, on

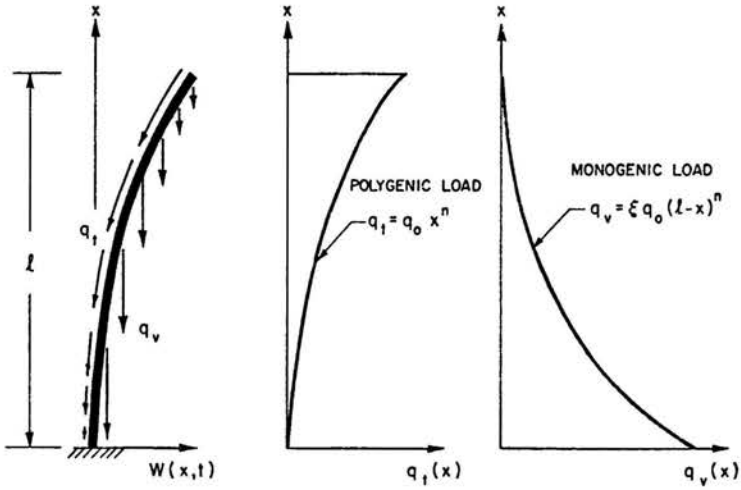

FIG. 1. The system.

the critical load and the mode of instability, is quite different in the subdomains $0 < \xi < \xi_D$, $\xi_D < \xi < \xi_F$ and $\xi_F < \xi < \infty$, where ξ_D and ξ_F are the critical values of ξ. The above subdomains are classified in gradually reducing proportion of polygenic forces.

2. The system and characteristic equations

The differential equation of small vibrations for the system, in Fig. 1, is obtained [9] as:

$$EIW_{xxxx}+\gamma W_{txxxx}+q_0(n+1)^{-1}\{[(l^{n+1}-x^{n+1}) + \xi(l-x)^{n+1}]W_{xx}-\xi(n+1)(l-x)^n W_x\}+\varrho W_{tt}=0 \tag{2.1}$$

along with the boundary conditions

$$\begin{aligned} W(0,t) &= W_x(0,t) = 0, \\ EIW_{xx}(l,t)+\gamma W_{txx}(l,t) &= EIW_{xxx}(l,t)+\gamma W_{txxx}(l,t) = 0, \end{aligned} \tag{2.2}$$

where ϱ is the linear mass density, E the Young's modulus, I the second moment of the cross-section and the subscripts denote the variables with respect to which the partial derivatives are taken. Introducing the nondimensional parameters

$$\begin{aligned} \eta = x(l)^{-1}, \quad \tau &= (EI)^{\frac{1}{2}}(\varrho l^4)^{-\frac{1}{2}}t, \quad G = (\varrho EIl^4)^{-\frac{1}{2}}\gamma, \\ F &= q_0 l^{n+3}[(n+1)EI]^{-1} \end{aligned} \tag{2.3}$$

and seeking the standing wave solution in the form

$$W(\eta, \tau) = e^{\omega\tau}\Phi(\eta), \tag{2.4}$$

where $\omega = \omega_R + j\omega_I$ is the complex frequency of vibration, yields the following non-self-adjoint boundary eigenvalue problem

$$(1+{}_{\omega}G)\Phi_{\eta\eta\eta\eta} + F\{[(1-\eta_1^{n+1}) + \xi(1-\eta)^{n+1}]\Phi_{\eta\eta} - \xi(n+1)(1-\eta)^n\Phi_{\eta}\} + \omega^2\Phi = 0, \tag{2.5}$$

$$\Phi(0) = \Phi_{\eta}(0) = \Phi_{\eta\eta}(1) = \Phi_{\eta\eta\eta}(1) = 0. \tag{2.6}$$

In the absence of the existence of a closed form solution for the above fourth-order system, we seek the solution

$$\Phi(\eta) = \sum_{r=1}^{\alpha} A_r \psi_r(\eta), \tag{2.7}$$

where $\psi_r(\eta's)$ are the orthogonal eigenfunctions of free vibrations of the system, obtained from Eqs. (2.5) and (2.6) by putting $F = G = 0$. Applying the Galerkin's method by substituting Eq. (2.7) in Eq. (2.5), taking $\alpha = 2$ and seeking nontrivial solution in A_r, yields the characteristic equation(1):

$$\omega^4 + \beta_1^*\omega^3 + \beta_2^*\omega^2 + \beta_3^*\omega + \beta_4^* = 0. \tag{2.8}^*$$

3. The instability boundary

The complex frequency of vibration, ω, decides on the state of the system. Inequality $\omega_R < 0$ implies asymptotic stability and $\omega_R > 0$, instability. The condition $\omega_R = 0$ represents entirely different phases for the damped and undamped systems. For the former it implies "instability boundary" and for the latter "stable domain or instability boundary". The imaginary component of the frequency, ω_I, governs the vibrational behaviour of the system. The conditions, $\omega_I \neq 0$ and $\omega_I = 0$, imply oscillatory and non-oscillatory motions, respectively. If at $\omega_R = 0^+$ ω_I is also zero, the system fails by divergence. If at $\omega_R = 0^+$, $\omega_I \neq 0$, the system fails by flutter. Therefore, the nondimensional critical load, K_{cr}, of the system, for a prescribed ξ, G and n, given by

$$K_{cr} = (1+\xi)F \tag{3.1}$$

is obtained, when the infinitesimal increase in F results, in the condition $\omega_R = 0^+$, for the first time.

For the undamped system, $\beta_1^* = \beta_3^* = 0$ in Eq. (2.8), and the divergence loads $\tilde{\tilde{K}}_{cr_D}$, corresponding to $\omega = 0$, are given by

$$\tilde{\tilde{K}}_{cr_{D(1,2)}} = (1+\xi)\tilde{M}_1[-1 \pm (1-\tilde{M}_2)^{\frac{1}{2}}]. \tag{3.2}^*$$

The flutter loads of the undamped system $\tilde{\tilde{K}}_{cr_F}$, corresponding to $\omega^2 \to$ complex, gives

$$\tilde{\tilde{K}}_{cr_{F(1,2)}} = (1+\xi)\tilde{M}_3[-1 \pm (1-\tilde{M}_4)^{\frac{1}{2}}]. \tag{3.3}^*$$

(1) Henceforth, equations superscripted ()* involve complicated mathematical expressions, in this case β_i^*, which for the sake of brevity are omitted here but explained in [9].

The criteria for the existence of the divergence and flutter loads of the undamped system are obtained as

$$\tilde{\tilde{\xi}}_{D(1,2)} \geqslant \tilde{T}_2(2\tilde{T}_1)^{-1}\{-1 \pm [1-4\tilde{T}_1\tilde{T}_3(\tilde{T}_2^2)^{-1}]^{\frac{1}{2}}\} \tag{3.4}*$$

and

$$\tilde{\tilde{\xi}}_{F(1,2)} \leqslant \tilde{\tilde{T}}_2(2\tilde{\tilde{T}}_1)^{-1}\{-1 \pm [1-4\tilde{\tilde{T}}_1\tilde{\tilde{T}}_3(\tilde{\tilde{T}}_2^2)^{-1}]^{\frac{1}{2}}\}, \tag{3.5}*$$

respectively.

For the damped system, the inequality

$$\beta_1^*(\beta_2^*\beta_3^* - \beta_1^*\beta_4^*) - \beta_3^{*2} > 0 \tag{3.6}$$

decides on the flutter loads, $\tilde{K}_{cr_F}$, which are obtained as

$$\tilde{K}_{cr_{F(1,2)}} = (1+\xi)\tilde{U}_1[-1 \pm (1-\tilde{U}_2)^{\frac{1}{2}}]. \tag{3.7}*$$

The divergence load of the damped system, $\tilde{K}_{cr_D}$, is given by the inequality

$$\beta_4^* > 0, \tag{3.8}$$

which leads to the same values as given by Eqs. (3.2) and (3.4). The criterion for the existence of flutter loads of the damped system is obtained as

$$\tilde{\xi}_{F(1,2)} \leqslant \Delta_{10}^*[-1 \pm (1-\Delta_{11}^*)^{\frac{1}{2}}]. \tag{3.9}$$

The lowest flutter and divergence loads for the damped system are given by $\tilde{K}_{cr_{F(1)}}$ and $\tilde{K}_{cr_{D(1)}}$, respectively; and the type of instability is governed by the lower of these two critical values. The transitional value of Kelvin-Voigt material damping G_t, at which the transition from flutter to divergence, if any, takes place, is obtained from the condition, $\tilde{K}_{cr_{F(1)}} = \tilde{K}_{cr_{D(1)}}$, which yields the *transition governing condition*

$$\tilde{\beta}_1(\xi, G)\{-1 + [1-\tilde{\beta}_2(\xi, G)]^{\frac{1}{2}}\} - \tilde{\beta}_3(\xi)\{-1 + [1-\tilde{\beta}_4(\xi)]^{\frac{1}{2}}\} = 0. \tag{3.10}*$$

4. The numerical analysis and discussion of the results

The authors have already shown [9, 10] that a change in the mode of instability from flutter to divergence for this class of systems, purely as the result of material damping, may be possible if the load distribution exponent satisfies the inequality

$$2.006 < n < \infty. \tag{4.1}$$

Taking the illustrative system as a viscoelastic steel cantilever of diameter 1 inch, length 50 in., and $n = 4$, results obtained on the IBM 360 computer of the University of Waterloo are plotted in Figs. 2–10. These shall be discussed at length.

4.1. The undamped system

The divergence and flutter boundaries of the undamped system, in the $\tilde{\tilde{K}}_{cr} - \xi$ plane, as obtained from Eqs. (3.2) and (3.3), are plotted in Fig. 2, where $\xi_D = 3.292747$ and $\xi_F = 4.175263$ are the positive critical values obtained from Eqs. (3.4) and (3.5), respectively. The following features are observed in Fig. 2:

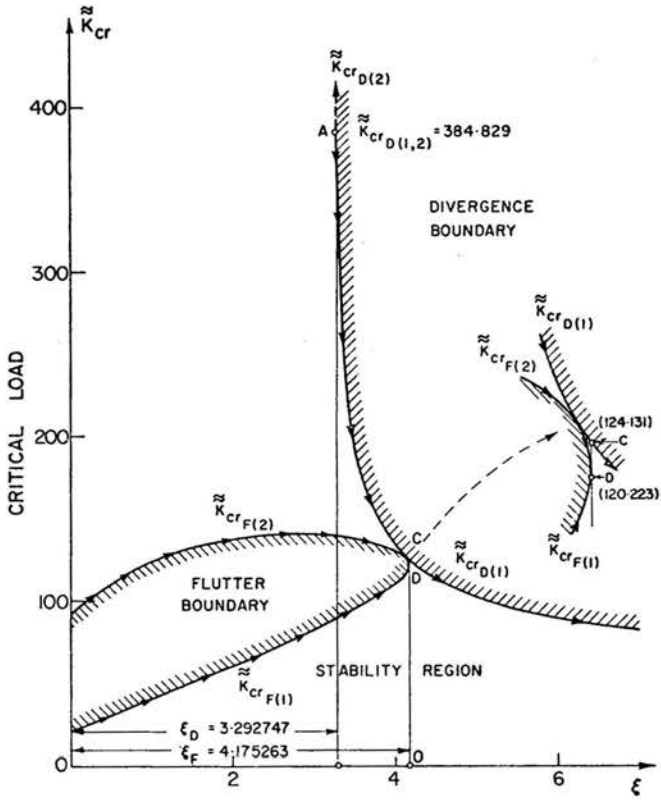

FIG. 2. The flutter-divergence boundaries of the undamped system.

i) *Range* $0 \leqslant \xi < \xi_D$. There exist two flutter loads such that $\tilde{\tilde{K}}_{cr_{F(1)}} < \tilde{\tilde{K}}_{cr_{F(2)}}$

ii) $\xi = \xi_D$. The introductory divergence load $\tilde{\tilde{K}}_{cr_{D(1,2)}} = 384.829$ appears at A such that $\tilde{\tilde{K}}_{cr_{F(1)}} < \tilde{\tilde{K}}_{cr_{F(2)}} < \tilde{\tilde{K}}_{cr_{D(1,2)}}$.

iii) *Range* $\xi_D < \xi < \xi_F$. There exist two flutter and two divergence loads such that $\tilde{\tilde{K}}_{cr_{F(1)}} < \tilde{\tilde{K}}_{cr_{F(2)}} < \tilde{\tilde{K}}_{cr_{D(1)}} < \tilde{\tilde{K}}_{cr_{D(2)}}$.

iv) $\xi = \xi_F$. There is coalescence of the two flutter loads at D such that $\tilde{\tilde{K}}_{cr_{F(1,2)}} = 120.223$. Besides, there exist two divergence loads, the lower being $\tilde{\tilde{K}}_{cr_{D(1)}} = 124.131$.

v) $\xi = \xi_F + \Delta\xi$. The flutter loads vanish and there is a transition in the mode of instability from kinetic to static. During this transition, the critical load jumps from $\tilde{\tilde{K}}_{cr_{F(1,2)}} = 120.223$ to $\tilde{\tilde{K}}_{cr_{D(1)}} = 124.131$. This jump(2) is represented by the vector DC.

vi) *Range* $\xi_F < \xi < \infty$. The system is purely divergent and $\tilde{\tilde{K}}_{cr_{D(1)}}$ is decisive for the critical load.

(2) The rare case where such a jump vanishes, occurs when n has the lower bound value in Eq. (4.1), [9, 10].

Conclusion I. The ratio of polygenic and monogenic forces ξ influences the mode of instability of the undamped system. An increase of ξ transforms the initial flutter system into a divergence system. This transformation occurs at $\xi = \xi_F$, accompanied by an abrupt increase of the critical load.

4.2. The damped system

The interaction between ξ and γ influences $\tilde{K}_{cr}$, the critical load of the damped system, as well as the mode of instability.

Figure 3 shows the mode separation curve *DAEF*, the vanishing flutter curve *DBECG* and the introductory divergence line *HEJ*, in the $\xi-\gamma$ plane. The introductory divergence

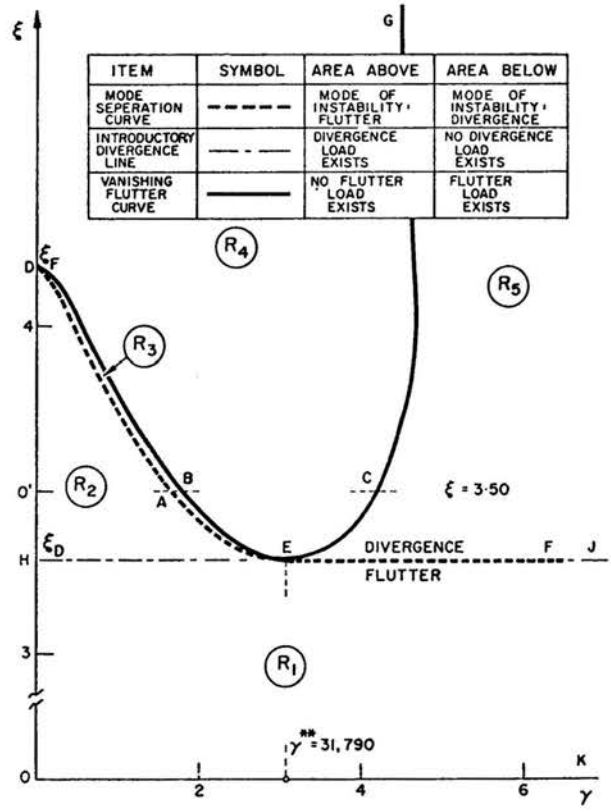

FIG. 3. The subspaces $R_1, \ldots, R_5$ of the damped system.

line, region *above*, which guarantees the existence of a divergence load, is obtained from Eq. (3.4). The vanishing flutter curve, region *below*, which guarantees the existence of a flutter load, is obtained from Eq. (3.9). The mode separation curve, regions above and below, which represent the divergence and flutter instability modes, respectively, is obtained from Eq. (3.10). The entire $\xi-\gamma$ plane is divided into five subspaces, R_i, which have distinct characteristics as explained in Table 1. The iso-ξ and iso-γ curves in the $\tilde{K}_{cr_F}-\gamma$ and

Table 1. The interpretation of subspaces R_i

Subspace	Range of ξ	Existence of critical load		Mode of instability
		F	D	
R_1	$0 < \xi < \xi_D$	Yes	No	F
R_2	$\xi_D < \xi < \xi_F$	Yes	Yes	F
R_3	$\xi_D < \xi < \xi_F$	Yes	Yes	D
R_4	$\xi_D < \xi < \infty$	No	Yes	D
R_5	$\xi_D < \xi < \infty$	Yes	Yes	D

F = Flutter; D = Divergence

$\tilde{K}_{cr_F} - \xi$ planes, as obtained from Eq. (3.7), and which ultimately lead to the optimal stability envelope, are shown in Figs. 4 and 5, respectively. The critical loads of systems with different ξ in the $\tilde{K}_{cr} - \gamma$ plane, as obtained from Eqs. (3.7) and (3.8), are shown in Figs. 6–10. The damped systems in ranges $0 < \xi < \xi_D$, $\xi_D < \xi < \xi_F$ and $\xi_F < \xi < \infty$ are discussed separately.

i) *Range* $0 < \xi < \xi_D$. This range, in Fig. 3, is represented by the rectangle *OHJK*, where only flutter instability is possible. The following features are observed in Figs. 4 and 5:

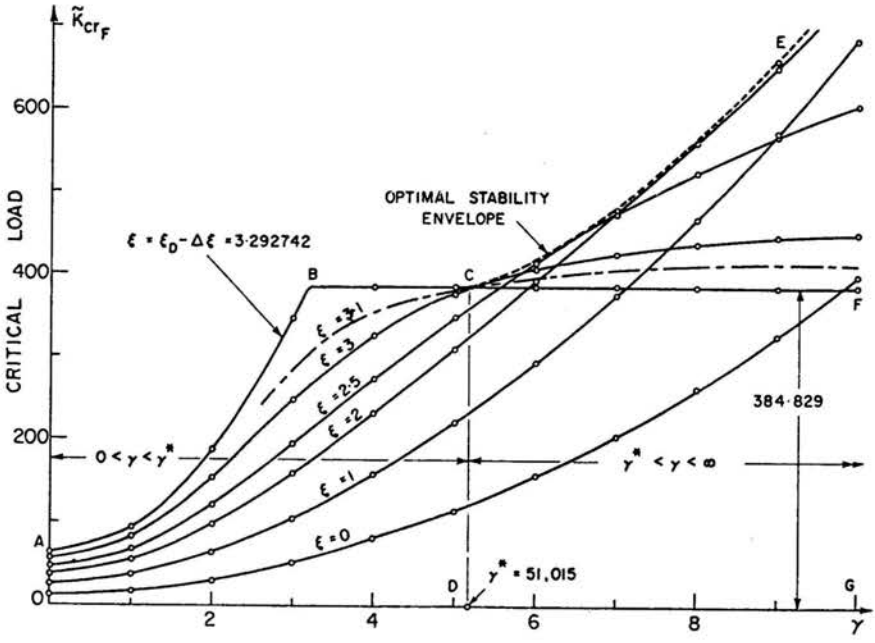

FIG. 4. The iso-ξ curves of the damped system.

a) in the range $0 < \gamma < \gamma^*$, represented by the area *OABCD* (Fig. 4), an increase in ξ raises the iso-ξ curves. Hence the increase of ξ increases the critical load.

b) in the range $\gamma^* < \gamma < \infty$, represented by the area *DCEFG* (Fig. 4), an increase in ξ up to a certain critical value increases the critical load, further increase in ξ lowers the critical

load. At $\xi \to \xi_D$, line CF, the flutter load attains its minima, $\tilde{K}_{cr_F} = 384.829$. For every γ, there exists a critical value of ξ which yields the maximum critical load. The optimal stability envelope contains all such maxima.

c) in the range $0 < \gamma < \gamma^*$, represented by the area $OAPQ$ (Fig. 5), all the iso-γ curves have a positive gradient. Hence, the increases of ξ increases the critical load.

d) in the range $\gamma^* < \gamma < \infty$, represented by the area above curve AP (Fig. 5), every iso-γ curve has an extremum. All such extrema are contained in the optimal stability envelope.

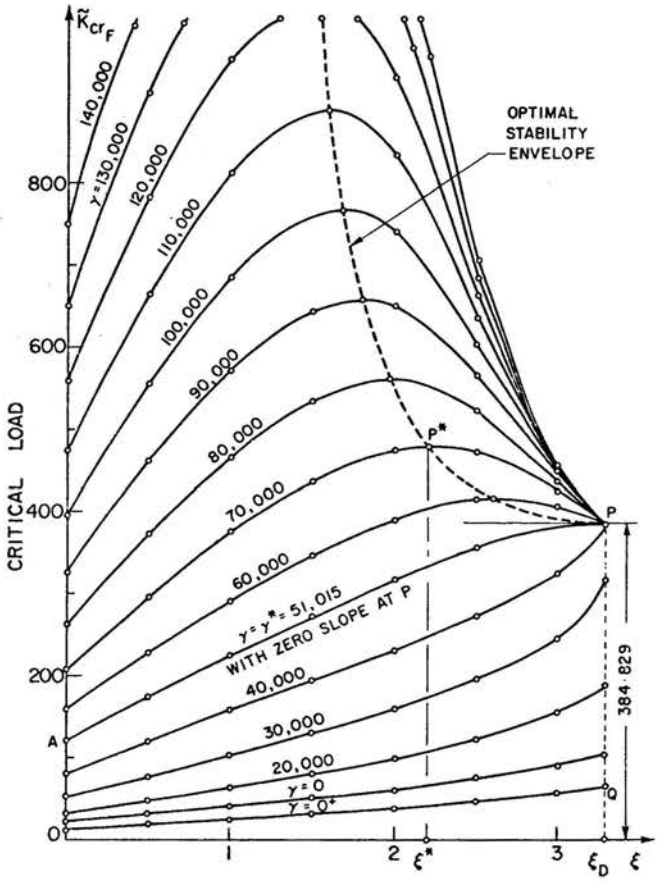

FIG. 5. The iso-γ curves of the damped system.

For a prescribed γ, the increase of ξ, up to a certain critical value ξ^*, increases the critical load. Any further increase of ξ reduces the critical load. Finally, as $\xi \to \xi_D$, all the iso-γ curves converge at P, yielding the flutter load $\tilde{K}_{cr_F} = 384.829$. The intersection between the optimal stability envelope and the prescribed iso-γ curve, P^*, yields the corresponding ξ^*.

ii) $\xi = \xi_D - \Delta\xi$. In Fig. 3, these systems belong to the region just below the line $HEFJ$. Since the mode separation curve is common with the introductory divergence line along EFJ, the flutter systems in the range $\gamma^{**} < \gamma < \infty$ are at the verge of becoming divergence

systems. This region, in Fig. 6, is represented by the area *SQRT*. In striking contrast to the area *OP'QS*, where the flutter loads, as expected, are highly sensitive to the material damping, the flutter load in the region *SQRT* remains constant.

iii) $\xi = \xi_D$. In Fig. 3, the line *HEFJ* represents this class of systems. In the range $\gamma^{**} < \gamma < \infty$, line *EFJ*, there exist both the divergence and flutter loads; and the mode

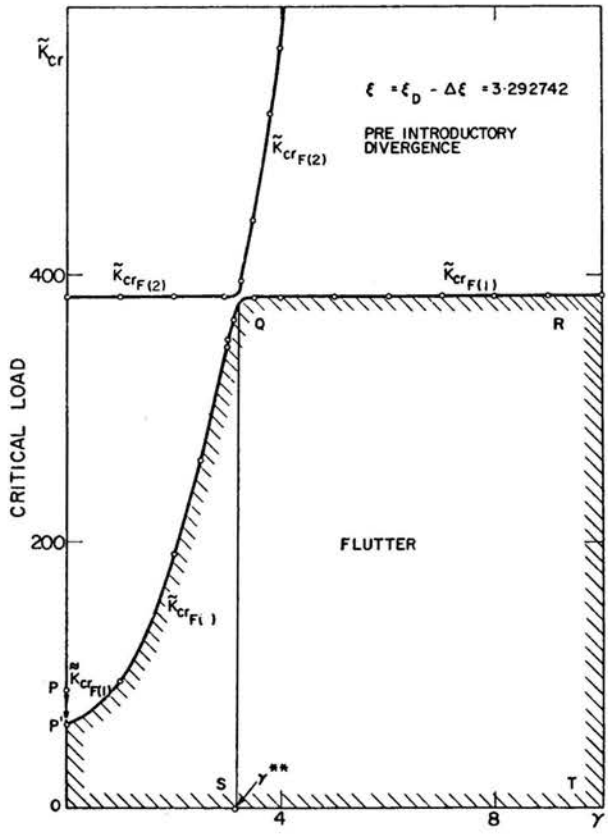

FIG. 6. The instability boundaries of the system $\xi = \xi_D - \Delta\xi$.

of instability is under a process of transition from flutter to divergence. This is clear from Fig. 7, where line *QR* represents the coincidental divergence and flutter loads, $\tilde{K}_{cr_{D(1)}}$ and $\tilde{K}_{cr_{D(1)}}$.

iv) $\xi = \xi_D + \Delta\xi$. In Fig. 3, a line parallel to and just above *HEFJ*, represents this class of systems. It can be visualized that the latter half of this line lies above the portion *EF* of the mode separation curve, and therefore these systems undergo the transition from flutter to divergence at a certain damping, $\gamma = \gamma_t$. The following features are observed in Fig. 8:

a) With the introduction of damping, the flutter load of the undamped system *OP* reduces to *OP'* due to the Ziegler's jump *PP'*.

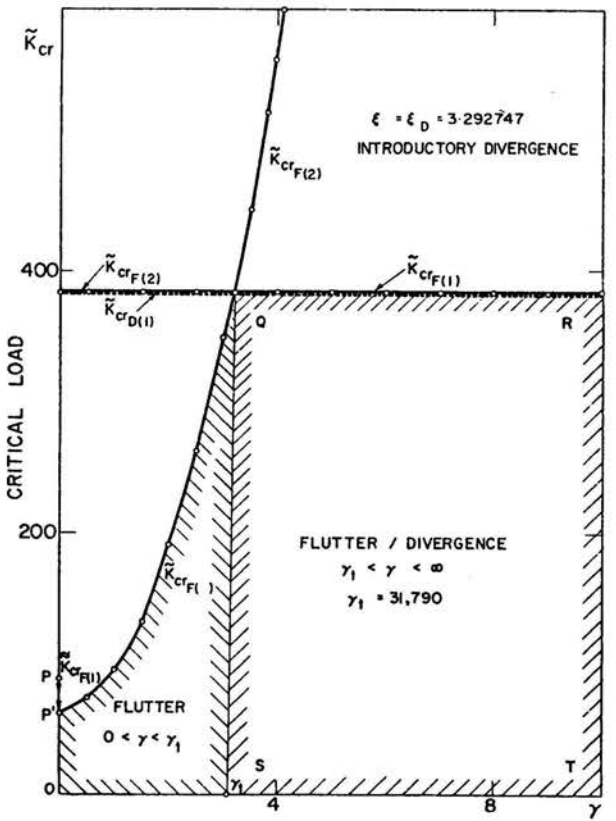

FIG. 7. The instability boundaries of the system $\xi = \xi_D$.

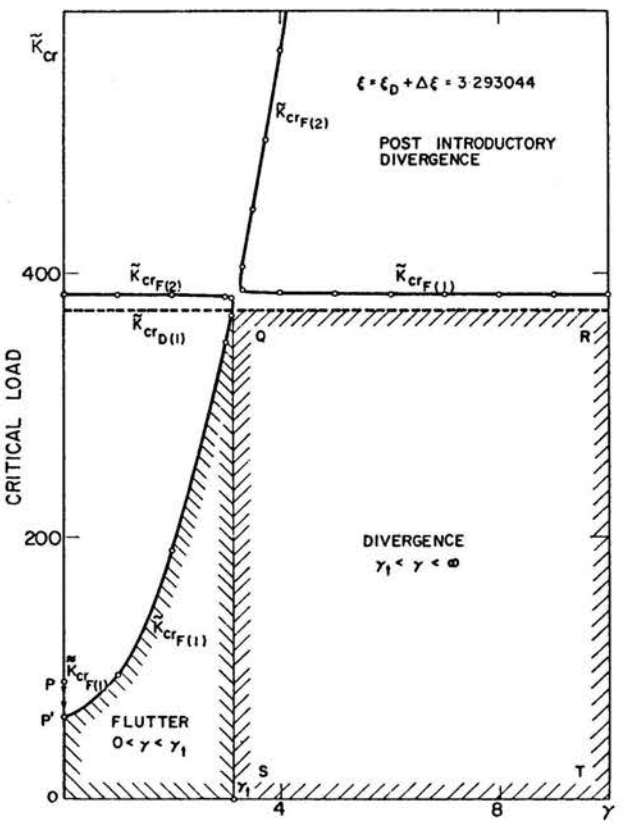

FIG. 8. The instability boundaries of the system $\xi = \xi_D + \Delta\xi$.

b) addition of damping, in the range $0 < \gamma < \gamma_t$, increases the critical load monotonically.

c) at $\gamma = \gamma_t$, the flutter load $\tilde{K}_{cr_{F(1)}}$ and the divergence load $\tilde{K}_{cr_{D(1)}}$ are identical at Q.

d) at $\gamma = \gamma_t + \Delta\gamma$, the mode of instability changes from flutter to divergence.

e) in the range $\gamma_t < \gamma < \infty$, area $SQRT$, the system continues to remain a divergence system with the critical load $\tilde{K}_{cr_{D(1)}}$.

v) *Range* $\xi_D < \xi < \xi_F$. This range in Fig. 3 is represented by the subspaces R_2 and R_3 in entirety, and the lower half of the subspaces R_4 and R_5. Since the portion DAE of the mode separation curve divides the subspaces R_2 and R_3 in the range $0 < \gamma < \gamma^{**}$, it is possible for the material damping, in the above range, to change the mode of instability of the system from flutter to divergence. For example, the system with $\xi = 3.50$, represented by the dotted line $O'ABC$, is a flutter system in the range $0 < \gamma < O'A$ and a diver-

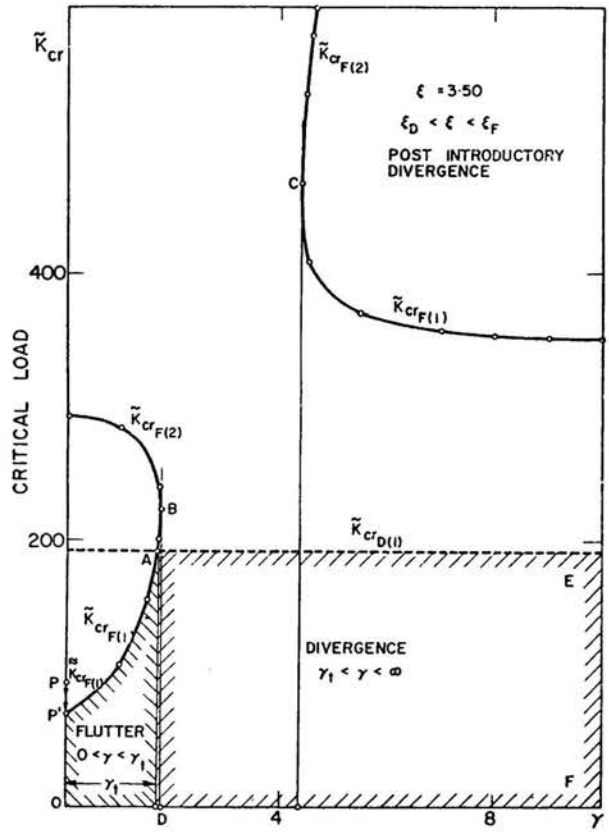

FIG. 9. The instability boundaries of the system $\xi = 3.50$.

gence system in the range $O'A < \gamma < \infty$; the transitional damping coefficient being $\gamma_t = O'A$. Figure 9, also representing the system $\xi = 3.50$, reveals the following features:

a) with the introduction of material damping, the flutter load of the undamped system OP reduces to OP' due to the Ziegler's jump PP'.

b) in the range $0 < \gamma < \gamma_t$, area $OP'AD$, addition of damping increases the flutter load monotonically.

c) in the range $\gamma_t < \gamma < \infty$, area $DAEF$, the system becomes divergent with the critical load $\tilde{K}_{cr_{D(1)}}$.

d) the damping values corresponding to A, B and C are identical to the values represented by A, B and C in Fig. 3.

vi) $\xi_F < \xi < \infty$. This range, in Fig. 3, is represented by the upper portion of subspaces R_4 and R_5. Since this area is above the mode seperation curve in entirety, the mode of instability remains as divergence. These are the so-called pseudo conservative systems, i.e., systems for which instability occurs through divergence, although at least some polyge-

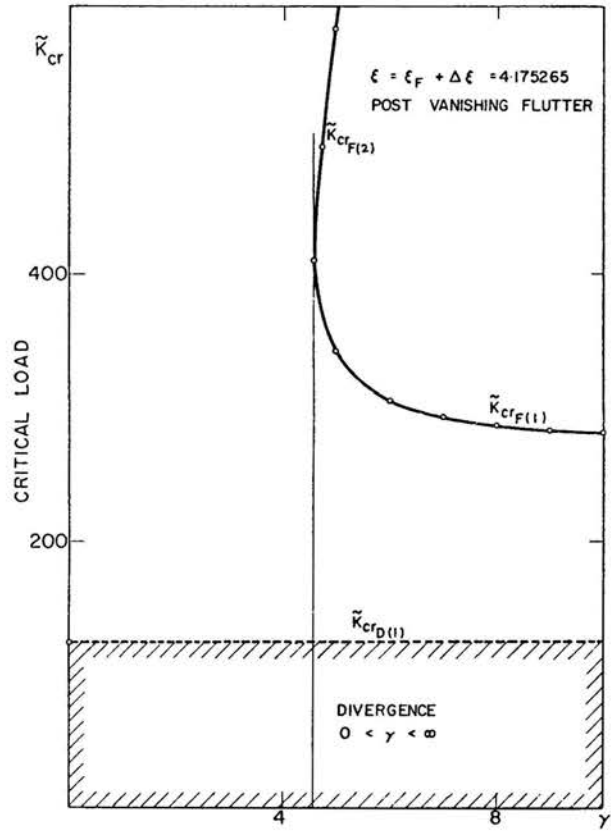

FIG. 10. The instability boundaries of the system. $\xi = \xi_F + \Delta\xi$

nic forces are present. A restudy of Figs. 7, 8 and 9 and Fig. 10, which represents the system $\xi = \xi_F + \Delta\xi_F$, reveals the following features:

a) an increase of ξ lowers the dotted divergence boundary, $\tilde{K}_{cr} = \tilde{K}_{cr_{D(1)}}$.

b) with the increase of ξ, the left and right loops of the flutter boundaries begin to shift apart. Finally, as seen in Fig. 10, the left loop of the flutter boundary disappears completely; rendering the system fully divergent.

Conclusion II. As a result of the interaction between ξ, the ratio of the polygenic and monogenic forces, and γ, the material damping coefficient; the mode of instability and the critical load of the damped system are influenced in the following manner:

i) in the range, $0 < \xi < \xi_D$, the mode of instability, which is flutter, remains unaltered. The critical load, however, is influenced significantly and the maximum attainable value is given by the optimal stability envelope.

ii) in the range, $\xi_D < \xi < \xi_F$, the transformation from flutter to divergence is possible at $\gamma = \gamma_t$ provided the inequality, $0 < \gamma < \gamma^{**}$, is satisfied. For $\gamma > \gamma^{**}$, the mode of instability becomes divergence. For $0 < \gamma < \gamma^{**}$, when the initial mode of instability is flutter, the critical load is influenced in the following manner: First, the introduction of infinitesimal damping produces the Ziegler's jump. Further addition of damping increases the critical load monotonically up to $\gamma = \gamma_t$, where the system transforms into a divergence system and the critical load thereafter remains constant. In contrast to the undamped case, there is no jump of the critical load during transformation from flutter to divergence.

iii) In the range, $\xi_F < \xi < \infty$, the mode of instability, which is divergence, remains unaltered. The critical load, as expected, remains insensitive to damping.

Acknowledgement

This research was supported by the National Research Council of Canada under Grant No. A-7297.

References

1. C. LANCZOS, *The variational principles of mechanics*, University of Toronto Press, Toronto, Fourth Edition, 30–31, 1970.
2. G. IU. DZHANELIDZE, *On the stability of a bar under the action of a follower force*, Transactions of Leningrad Politekhn. In-Ta, 192, 1958.
3. KÖNIG, *Die Knickkraft beim Einseitig eingespannten Stab unter nichtrichtungstreuer Kraftwirkung*, Der Stahlbau, **29**, 150, 1960.
4. H. ZIEGLER, *Principles of structural stability*, Blaisdell Publishing Co., London, First Edition, 114–115, 1968.
5. G. HERRMANN, and R. W. BUNGAY, *On the stability of elastic systems subjected to nonconservative forces*, J. Appl. Mech., **31**, 3, 435–440, 1964.
6. M. ŻYCZKOWSKI, and A. GAJEWSKI, *Optimal structural design in nonconservative problems of elastic stability, in* "Instability of Continuous Systems", IUTAM Symposium 1969, Edited by H. H. E. LEIPHOLZ, Springer-Verlag, First Edition, 295–301, 1971.
7. K. HUSSEYIN, and R. H. PLAUT, *The elastic stability of two-parameter nonconservative systems*, Solid Mechanics Division, Paper No. 91, University of Waterloo, 1971.
8. V. V. BOLOTIN, and N. I. ZHINZHER, *Effects of damping on stability of elastic systems subjected to nonconservative forces*, Int. J. Solids and Structures, **5**, 9, 965–989, 1969.
9. H. H. E. LEIPHOLZ, and R. KAPOOR, *Influence of Kelvin model damping in flutter-divergence transitional polygenic systems*, Solid Mechanics Division Paper No. 110, University of Waterloo, March 1972.
10. R. N. KAPOOR, and H. H. E. LEIPHOLZ, *Flutter-divergence transition criteria in certain viscoelastic polygenic systems*, Proc. 13th Mitwestern Mech. Conf., Pittsburg 1973.

HATCH ASSOCIATES LIMITED TORONTO, CANADA
nnd
SOLID MECHANICS DIVISION, FACULTY OF ENGINEERING, UNIVERSITY OF WATERLOO.

Received May 3, 1973.